SVN Stroke & Vascular Neurology

APE1 regulates mitochondrial DNA damage repair after experimental subarachnoid haemorrhage in vivo and in vitro

Kun Dai,[1,2] Zongqi Wang,[1,2] Bixi Gao,[1,2] Longyuan Li,[1,2] Feng Gu,[1,2] Xinyu Tao,[1,2] Wanchun You,[1,2] Zhong Wang [1,2]

To cite: Dai K, Wang Z, Gao B, *et al*. APE1 regulates mitochondrial DNA damage repair after experimental subarachnoid haemorrhage in vivo and in vitro. *Stroke & Vascular Neurology* 2024;**9**: e002524. doi:10.1136/svn-2023-002524

► Additional supplemental material is published online only. To view, please visit the journal online (http://dx.doi.org/10.1136/svn-2023-002524).

KD and ZW contributed equally.
WY and ZW contributed equally.

Received 12 April 2023
Accepted 9 August 2023
Published Online First 23 August 2023

[1]Department of Neurosurgery & Brain and Nerve Research Laboratory, First Affiliated Hospital of Soochow University, Suzhou, Jiangsu, China
[2]Institute of Stroke Research, Soochow University, Suzhou, Jiangsu, China

Correspondence to
Professor Zhong Wang; wangz8761@163.com

Dr Wanchun You; wcyou@suda.edu.cn

ABSTRACT

Background Subarachnoid haemorrhage (SAH) can result in a highly unfavourable prognosis. In recent years, the study of SAH has focused on early brain injury (EBI), which is a crucial progress that contributes to adverse prognosis. SAH can lead to various complications, including mitochondrial dysfunction and DNA damage. Apurinic/apyrimidinic endonuclease 1 (APE1) is an essential protein with multifaceted functionality integral to DNA repair and redox signalling. However, the role of APE1 in mitochondrial DNA damage repair after SAH is still unclear.

Methods Our study involved an in vivo endovascular perforation model in rats and an in vitro neuron oxyhaemoglobin intervention. Then, the effects of APE1 on mitochondrial DNA damage repair were analysed by western blot, immunofluorescence, quantitative real-time PCR, mitochondrial bioenergetics measurement and neurobehavioural experiments.

Results We found that the level of APE1 decreased while the mitochondria DNA damage and neuronal death increased in a rat model of SAH. Overexpression of APE1 improved short-term and long-term behavioural impairment in rats after SAH. In vitro, after primary neurons exposed to oxyhaemoglobin, APE1 expression significantly decreased along with increased mitochondrial DNA damage, a reduction in the subunit of respiratory chain complex levels and subsequent respiratory chain dysfunction. Overexpression of APE1 relieved energy metabolism disorders in the mitochondrial of neurons and reduced neuronal apoptosis.

Conclusion In conclusion, APE1 is involved in EBI after SAH by affecting mitochondrial apoptosis via the mitochondrial respiratory chain. APE1 may potentially play a vital role in the EBI stage after SAH, making it a critical target for treatment.

WHAT IS ALREADY KNOWN ON THIS TOPIC

⇒ Subarachnoid haemorrhage is a type of haemorrhagic stroke caused by intracerebral aneurysm rupture, resulting in irreversible consequences. The development of early brain injury following subarachnoid haemorrhage is a multifaceted pathological process that involves both direct injury and subsequent pathophysiological alterations in the brain within 72 hours. The mechanisms of early brain injury may be associated with oxidative stress, inflammation, apoptosis and DNA damage.

WHAT THIS STUDY ADDS

⇒ Our research first confirmed that the involvement of APE1 in the mitochondrial respiratory chain-mediated mitochondrial apoptosis pathway in the development of early brain injury following subarachnoid haemorrhage.

HOW THIS STUDY MIGHT AFFECT RESEARCH, PRACTICE OR POLICY

⇒ Our research clarified targeting APE1 could be a promising therapeutic strategy for the management of early brain injury following subarachnoid haemorrhage.

INTRODUCTION

Subarachnoid haemorrhage (SAH) is a type of haemorrhagic stroke caused by intracerebral aneurysm rupture, resulting in irreversible consequences.[1 2] Given the high mortality and morbidity rates associated with SAH, extensive research has been conducted to elucidate the molecular mechanisms underlying this severe medical condition.[3 4] In recent years, the study of SAH has focused on early brain injury (EBI), which is a crucial progress that contributes to adverse prognosis in SAH patients.[5] The development of EBI following SAH is a multifaceted pathological process that involves both direct injury and subsequent pathophysiological alterations in the brain within 72 hours. The mechanisms of EBI may be associated with oxidative stress, inflammation, apoptosis and DNA damage.[5–7]

Oxidative DNA damage is a well-recognised consequence of oxidative stress in EBI after SAH.[8–10] Failure to repair DNA damage results in the activation of multiple pathways that induce cell death, including apoptosis, senescence and autophagy. The mammalian cell contains two genomes: nuclear DNA (nDNA) and mitochondrial DNA (mtDNA). nDNA and mtDNA are continuously at risk of

suffering oxidative DNA damage. Compared with nDNA, mtDNA is more susceptible to alteration.[11] Since the mitochondrial inner membrane is the primary source of intracellular reactive oxygen species, mtDNA constantly suffers from oxidative DNA damage. Moreover, mtDNA lacks protective histones and efficient DNA repair capacity.[12] To deal with the damage, mitochondria are forced to effectively repair the DNA lesion using its endogenous DNA repair machinery.[13] Base excision repair (BER) is the principal mechanism for repairing oxidative DNA damage in eukaryotic cells, specifically within the mitochondrial genome.

Human apurinic/apyrimidinic endonuclease 1 (APE1) is an essential protein with multifaceted functionality integral to DNA repair and redox signalling.[14] As a critical DNA repair enzyme, it is crucial in both nuclear and mitochondrial BER pathways. In addition to playing a vital role in mammals since early embryonic development, knockout of APE1 results in embryonic lethality.[15] APE1 cleaves the DNA backbone as an endonuclease enzyme, generating 5′-phosphate and 3′-hydroxyl ends, restoring the original base pair by DNA polymerase β.[16]

Recent research has emphasised the significance of DNA repair in the intrinsic brain repair mechanism during the recuperation phase after a stroke. This research aims to comprehensively explore the role of APE1 in mtDNA damage repair after SAH.

METHODS AND MATERIALS

Experimental animals

During the experiment, the rats were subjected to feeding, utilisation, and surgical procedures that strictly adhered to the regulations set forth for the protection of experimental animals. Sprague Dawley (SD) rats, which are healthy adult males weighing between 280 and 320 g and aged between 8 and 12 weeks, have been procured from the Animal Center of the Chinese Academy of Sciences (Shanghai, China). Pregnant SD rats (pregnant 16–18 days) were used to prepare primary-neuron-enriched cultures. A total of 327 rats were included in this work, and the animal group administration was performed following randomised, controlled and double-blind principles. Animals in each group were assessed in a double-blind manner, and the investigators were blinded to the animal's serial number and experimental group. Every possible measure was taken to minimise the suffering of the animals during the experiments. All animal research data are written according to Animal Research: Reporting of in vivo Experiments guidelines.

Experimental design

The representative images of the rat SAH model and the diagram of the experimental design are presented in online supplemental figure S1. The SAH grading score of experiment 1 and experiment 3 are presented in online supplemental figure S2.

Establishing the SAH model in vivo

The rat model for SAH using endovascular perforation (EVP) has been reported in previous studies.[17] Briefly, the SD rats were anaesthetised persistently by 2% isoflurane. Next, the right internal carotid artery is entered using a 4–0 sharpened single filament nylon via the right external carotid artery stump. The filament is then advanced until resistance is encountered, at which point it is further advanced by 2–3 mm before being withdrawn. Following this, the incision is sutured, and the SD rat is confined in isolation for 1 hour to undergo observation. Rats were placed supine on the operation table with a heating blanket to maintain body temperature during the procedure. After that, the SD rat is returned to the animal room for regular feeding. During rat sacrifice, SAH grade was conducted and the score ≥8 indicates successful modelling of SAH, whereas the score <8 was excluded from the study. The sham group underwent identical procedures but without puncturing the internal carotid artery. The mortality and exclusion rates of the EVP SAH model are detailed in online supplemental table S1.

Establishing the SAH model in vitro

As described previously, primary rat embryonic cortical neurons were prepared and cultured.[18] Brain tissues were digested with trypsin at 37°C for 8 min. Following the formation of brain tissue suspensions, centrifugation was performed at a speed of 1500 rpm for 5 min. The resultant cells were subsequently suspended in Neurobasal Medium, supplemented with 2% B27, 0.5 mM L-glutamine, 50 units/mL of penicillin and streptomycin, all procured from Gibco. Finally, neurons were seeded into 100 mm dishes at a density of 10^5 cells/cm^2 or 24-well plates at a density of 2×10^4 cells/cm^2, and the medium was changed with fresh medium every another day. Establishing an in vitro SAH model involved the exposure of cultured neurons to 10 µM oxygenated haemoglobin (OxyHb) for 12 hours at 37°C.

Transfection of adeno-associated virus in vivo and intracerebroventricular injection

An adeno-associated viral vector (AAV, promoter-MCS-EGFP-3FLAG-SV40, 6.51×10^{12}VG/mL) was used to overexpress rat APE1. The AAV-APE1 and negative AAV-CON 308 for rats with a serotype of AAV9 were purchased from Genechem Co. (Shanghai, China). The injection coordinates were set at 0.8 mm posterior, 1.5 mm right lateral and 3.7 mm ventral from Bregma. A volume of 5 µL of AAV was introduced into the right lateral ventricle. Following the injection, the anaesthetised rats were revived within 5 min. Successful transfection was achieved after a period of 21 days. Adeno-associated virus information in detail can be found in online supplemental table S2.

Plasmid transfection in neurons

According to the manufacturers' instructions, overexpression of APE1 plasmid was transfected by Lipofectamine2000 (Invitrogen). A 10 µL Lipofectamine2000

mixed with 4 µg plasmid DNA was used per well in a 6-well plate format for 48 hours. Lipofectamine2000 intervention was used as an internal control. APE1 overexpression plasmid information in detail can be found in online supplemental table S3.

Quantitative real-time PCR

The measurement of mtDNA and mtDNA 4834 bp (4.8 Kb) deletion was conducted through quantitative real-time PCR (qPCR) to determine their relative content.[19] The mtDNA 4.8 Kb deletion indicated structural harm to the mitochondrial genome.[20] The SYBR Green was used to perform reactions on a StepOne Plus Real-Time PCR System (Applied Biosystems). To ensure comprehensive analysis, each sample was tested three times. The testing was carried out in a final volume of 10 µL, comprising iTaq SYBR Green Supermix PCR 1×Master Mix (Bio-Rad Laboratories, Hercules, California, USA), 0.4 µM forward and reverse primers, and 2 ng DNA template. The reaction conditions were: 30 s of denaturation at 95 °C, followed by 40 cycles of 95 °C for 30 s, annealing and extension at 60 °C for 20 s. To estimate the quantification of the mtDNA content, we calculated the ratio of mtDNA to nDNA (β-actin) using the following formula: mtDNA content=$2^{-\Delta\Delta Ct}$.[21] The relative content of the 4.8 Kb deletion normalised to mtDNA content was calculated using the formula: 4.8 Kb deletion content=$2^{\Delta CTx}$ - $2^{\Delta CTb}$ (ΔCTx denotes the variation between the 4.8 Del CT values and mtDNA CT values, and ΔCTb indicates the variation between mtDNA CT values and β-actin CT values).[20] Table 1 displays the primer sequences.

Measurement of mitochondrial bioenergetics

To monitor the cellular oxygen consumption rate (OCR), the XF24 Flux Analyzer (Seahorse Bioscience, North Billerica, Massachusetts, USA) was employed following the manufacturer's instructions. The process commenced with the adherence of 1×10^4 primary neurons to an XF96 well plate. Subsequently, oligomycin (1 µM), carbonylcyanide-4-(trifluoromethoxy) phenylhydrazone (FCCP, 1 µM), rotenone (1 µM) and antimycin A (1 µM) were sequentially added to each well to measure the OCR (pMoles/min). The tests were repeated three times to validate the results.

Behavioural tests

Detailed methods of behavioural tests: modified Garcia score, beam balance test and balance beam walking test, and Morris Water Maze are presented in online supplemental material.

Statistic analysis

GraphPad V.9.0.0 (Prism) software was used to perform all statistical analyses, and the mean±SD values were reported for all data. Normal distribution and homogeneity of variance were examined first. Next, the results were analysed by appropriate tests. The comparison of two groups was conducted using Student's t-test, while the comparison of multiple groups was carried out using one-way ANOVA. A $p<0.05$ was considered as the difference was statistically significant. All specific statistical and exact p values can be found in online supplemental table S4.

RESULTS

Mitochondrial APE1 level decreased and mtDNA damage increased after SAH in vivo

The temporal cortex's mitochondria and cytoplasm were isolated through the utilisation of standard differential centrifugation procedures (figure 1A). We determined the purity of the isolated mitochondria through Western blot (figure 1B). In comparison to the sham group, the Western blot analysis revealed a significant decrease in the protein expression of APE1 in both the cytoplasm and mitochondria 24 hours post-SAH (figure 1C,D). At 48 hours after SAH, APE1 protein expression reached its lowest point. Additionally, we evaluated the overall and nuclear expression of APE1. The APE1 alteration in the nuclear and total cells was consistent with that in the mitochondria (online supplemental figure S3). The cerebral tissue samples of the sham and SAH 48-hour groups were examined in immunofluorescent staining. NeuN was used as neuron marker, and APE1/NeuN was colocalised. The results showed that the expression of APE1 decreased (figure 1E,F). The APE1/Tomm20 costaining results were consistent with that in APE1/NeuN staining (online supplemental figure S4).

We employed qPCR to determine both the relative content of mtDNA and mtDNA 4834 bp (4.8 Kb) deletion in the brains of subjects from both the sham and SAH groups. The result showed that the amount of mtDNA decreased after SAH (figure 1G). Meanwhile, the normalised content of the 4.8 Kb deletion concerning mtDNA content exhibited a significant increase following SAH (figure 1H).

Table 1 Oligonucleotide primer sequences

Primer set	Forward primer	Reverse primer	(nps)	(nps)
mtDNA	5'GGTTCTTACTTCAGGGCCATCA3'	5'TGATTAGACCCGTTACCATCGA3'	15 785–15 806	15 868–15 847
4.8 del	5'AAGGACGAACCTGAGCCCTAATA3'	5'CGAAGTAGATGATGCGTATACTGTA3'	8109–8131	13 020–12 996
β-actin	5'CCCAGCCATGTACGTAGCCA3'	5'CGTCTCCGGAGTCCATCAC3'	2181–2200	2266–2248

mtDNA, mitochondrial DNA.

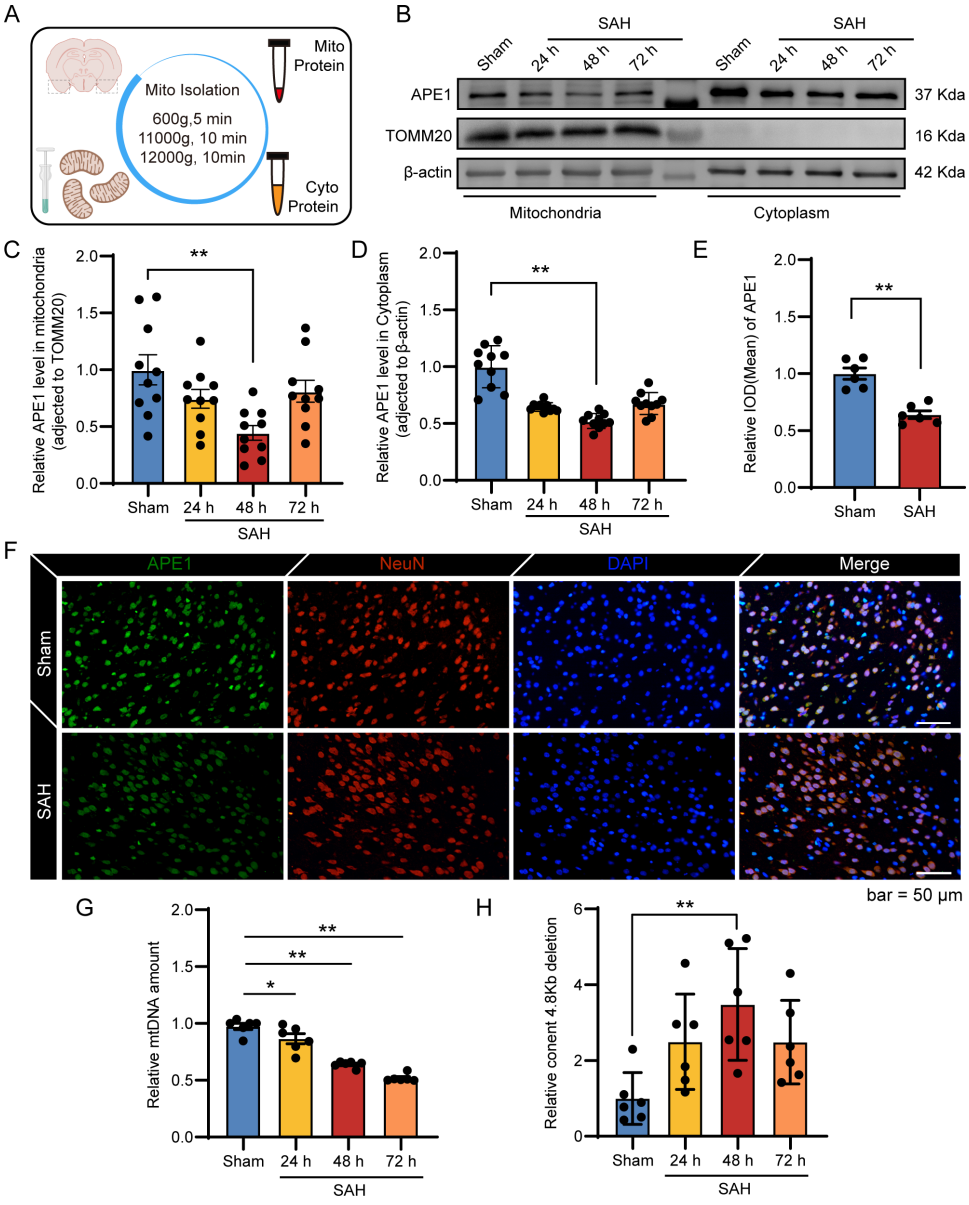

Figure 1 Mitochondrial APE1 level decreased and mtDNA damage increased after SAH in vivo. (A) Mitochondria and cytoplasm separated through centrifugation procedures. (B–D) The temporal pattern of APE1 expression in rat brain tissue after SAH both in mitochondria and cytoplasm. Tomm20 and β-actin serve as load control for mitochondria and cytoplasm, respectively. (C) Presents a quantitative assessment of the APE1 level in mitochondria. Sham versus SAH 48 hours, p=0.0008. (D) Presents a quantitative assessment of the APE1 level in the cytoplasm. Sham versus SAH 48 hours, p<0.0001. n=10 per group. (E, F) Colocalisation of APE1 (green), NeuN (red) and DAPI (blue) within brain temporal cortex tissue both of sham and SAH 48 hours group. Scale bar=50 μm. (E) Quantitatively assesses the APE1's IOD (mean). Sham versus SAH 48 hours, p=0.0001. n=6 per group. (G) Relative mitochondrial DNA (mtDNA) content in brain temporal cortex tissue from Sham, SAH 24 hours, SAH 48 hours and SAH 72 hours rats. Sham versus SAH 24 hours, p=0.0313. Sham versus SAH 48 hours, p<0.0001. Sham versus SAH 72 hours, p<0.0001. n=6 per group. (H) Relative content of mtDNA 4.8 Kb deletion in brain temporal cortex tissue from Sham, SAH 24 hours, SAH 48 hours and SAH 72 hours rats. Sham versus SAH 48 hours, p=0041. n=6 per group. The data are expressed in the form of mean±SD. * and ** denote statistical significance at p<0.05 and p<0.01, respectively. The abbreviation 'ns' indicates that there was no significant difference observed. SAH, subarachnoid haemorrhage.

Mitochondrial APE1 decreased and mtDNA damage increased after OxyHb intervention in vitro

To simulate SAH, primary neurons were cultured and subsequently exposed to OxyHb in an in vitro setting. Neuronal proteins were isolated and separated into their respective mitochondrion and cytoplasmic components for Western blot analysis. The findings indicated a notable reduction in the expression of APE1 in both the mitochondria and cytoplasm (figure 2A–C). In immunofluorescent staining, we used Tomm20 as a marker for mitochondria in the neuron. The results of our study indicated that the presence of OxyHb led to a notable decrease in APE1 protein expression in neurons (figure 2D,E). The relative expression level of the γ-H2AX was used as a marker of

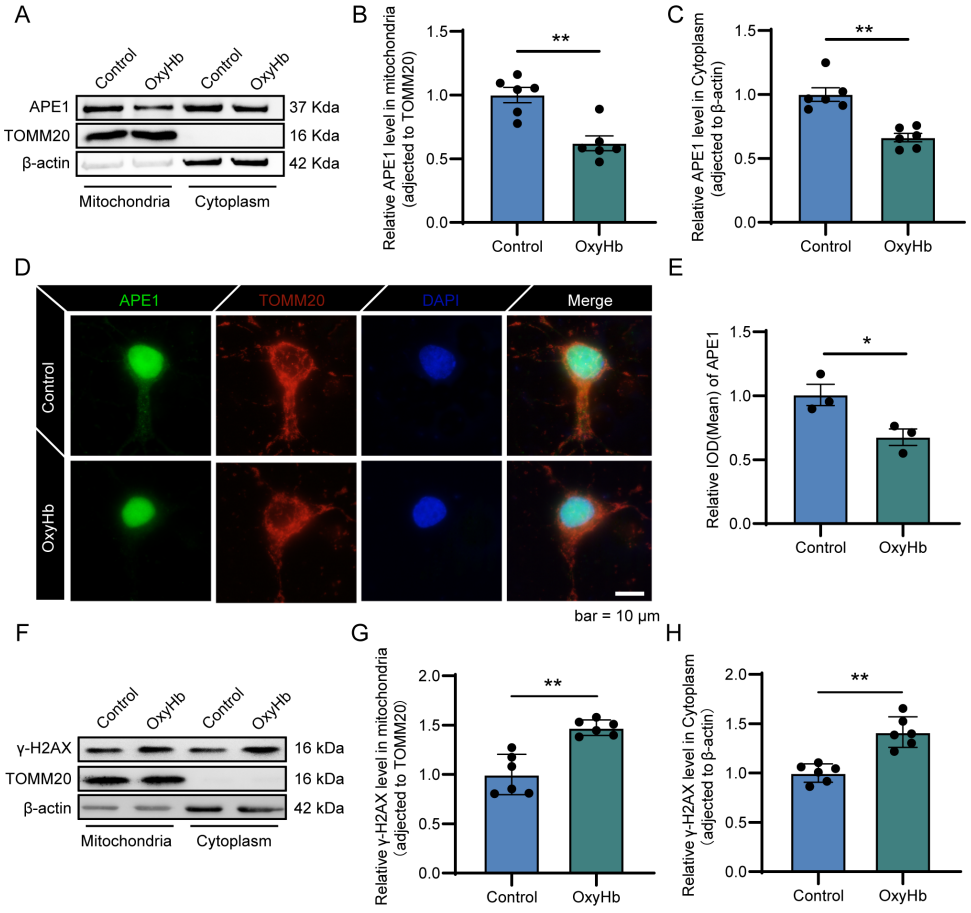

Figure 2 Mitochondrial APE1 decreased and mtDNA damage increased in vitro. (A–C) Expression changes of APE1 in the neurons of control and OxyHb groups. Tomm20 and β-actin serve as load control for mitochondria and cytoplasm, respectively. (B) Presents a quantitative assessment of the APE1 level in mitochondria. Control versus OxyHb, p=0.0011. (C) Presents a quantitative evaluation of the APE1 level in the cytoplasm. Control versus OxyHb, p=0.0003. n=6 per group. (D, E) Colocalisation of APE1 (green), Tomm20 (red) and DAPI (blue) within neurons both of control and OxyHb 12 hours group. Scale bar=10 μm. Figure E quantitatively assesses the APE1's IOD (mean). Control versus OxyHb, p=0.0344. n=3 per group. (F–H) Expression changes of γ-H2AX in the neurons of control and OxyHb groups, n=6 per group. Tomm20 and β-actin serve as load control for mitochondria and cytoplasm, respectively. Figure G presents a quantitative assessment of the γ-H2AX level in mitochondria. Control versus OxyHb, p=0.0003. (H) Presents a quantitative evaluation of the γ-H2AX level in the cytoplasm. Control versus OxyHb, p=0.0002. The data are expressed in the form of mean±SD. * and ** denote statistical significance at p<0.05 and p<0.01, respectively. OxyHb, oxygenated haemoglobin.

DNA damage. We found that the expression of γ-H2AX decreased in mitochondria and cytoplasm after exposure to OxyHb (figure 2F–H).

APE1 overexpression reduced neuronal apoptosis after SAH

We performed an overexpression experiment using AAV via intracerebroventricular injections. The overexpression effect was validated by Western blot. It was observed that the AAV-APE1 group exhibited a significant upregulation in the expression level of APE1 compared with the AAV-CON 308 group (figure 3A,B). After APE1 overexpression, we performed Nissl staining to examine neuronal injuries. The AAV-APE1 group exhibited a significant reduction in the number of Nissl bodies in rat brain sections after SAH in comparison to the AAV-CON 308 group (figure 3C,D).

Meanwhile, we determined the apoptosis-related protein cleaved-caspase 9 expression levels. Western blot analysis indicated that overexpression of APE1 led to a substantial reduction in the expression of cleaved-caspase 9 (figure 3E,F). Our results revealed that neuron apoptosis after SAH is possibly partly reduced by APE1 overexpression.

APE1 overexpression improved short-term and long-term neurological functions after SAH

To assess the impact of APE1 overexpression on the short-term and long-term neurobehavioral outcomes of the subjects, we conducted four behavioural examinations (figure 4A). Before establishing the SAH model, rats were trained to establish baseline performance. The balance beam test and modified Garcia scores of rats in the SAH group were notably inferior to those of the sham group, and AAV-APE1 injection could significantly increase the score (figure 4B,D). Moreover, in the balance beam walking test, the rats of the SAH group took significantly

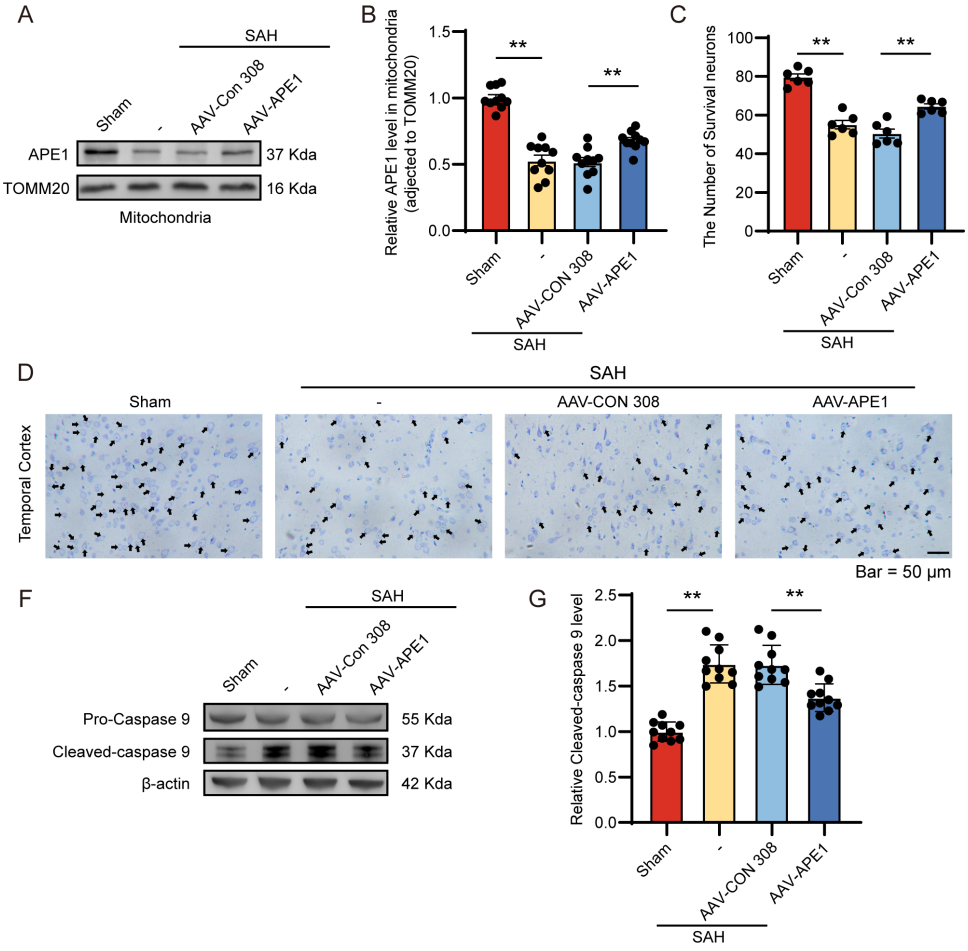

Figure 3 APE1 overexpression reduced neuronal apoptosis after SAH. (A, B) The effectiveness of APE1 overexpression through Western blot analysis. Tomm20 as load control. Figure B presents a quantitative assessment of the APE1 level in mitochondria. Sham versus SAH, p<0.0001. SAH+AAV CON 308 vs SAH+AAV-APE1, p=0.0015. n=10 per group. (C, D) Nissl staining of rat brain tissues and representative Nissl bodies is denoted by the arrows. Scale bar=50 µm. (D) Presents a quantitative assessment of the survival neuron number. Sham versus SAH, p<0.0001. SAH+AAV CON 308 vs SAH+AAV-APE1, p=0.0015. n=10 per group. (F) Caspase 9 and Cleaved-caspase 9 in vivo were performed by Western blot analysis. (G) Quantitative analysis of relative Cleaved-caspase9 protein levels, β-actin as load control. n=10 per group. Sham versus SAH, p<0.0001. SAH+AAV CON 308 vs SAH+AAV-APE1, p=0.0005. The data are expressed as mean±SD. * and ** denote statistical significance at p<0.05 and p<0.01, respectively. 'ns' indicates that there was no significant difference observed. AAV, adeno-associated viral vector; SAH, subarachnoid haemorrhage.

longer to cross the beam than the Sham group, and APE1 overexpression reduced the arrival time (figure 4C).

The Morris water maze test was conducted to evaluate spatial learning and long-term working memory. The swimming mean speed of the four groups was similar (figure 4E). There was a noticeable decrease in the escape time for all groups, with the rats in the SAH group taking a more extended period to locate the concealed platform in comparison to those in the sham group (figure 4F). The swimming distance of AAV-APE1 group was markedly shorter than that of the SAH and the SAH+AAV CON 308 group (figure 4G). Moreover, the overexpression of APE1 substantially enhanced the duration spent in the target quadrant, denoting an improvement in the persistent spatial learning and memory deficiencies triggered by SAH (figure 4H).

APE1 overexpression attenuated mitochondrial membrane potential impairment and neuronal apoptosis in vitro

Neurons were transfected with a plasmid that overexpressed APE1, and subsequently, the level of APE1 protein was determined via western blot analysis (figure 5A,B). We performed transmission electron microscope observation on the mitochondrial structure of primary neurons after APE1 intervention. Neuronal mitochondria in the control group were intact, and its crista was distributed evenly. The mitochondrial morphology of neurons in the OxyHb and OxyHb+Vector groups experienced destruction, with membrane and crista dissolution. Overexpression of APE1 attenuated mitochondria destruction (online supplemental figure S5). The outcomes revealed a significant elevation in the expression level of APE1 in the OE APE1 group compared with the vector group. We detected the ATP content in neurons to

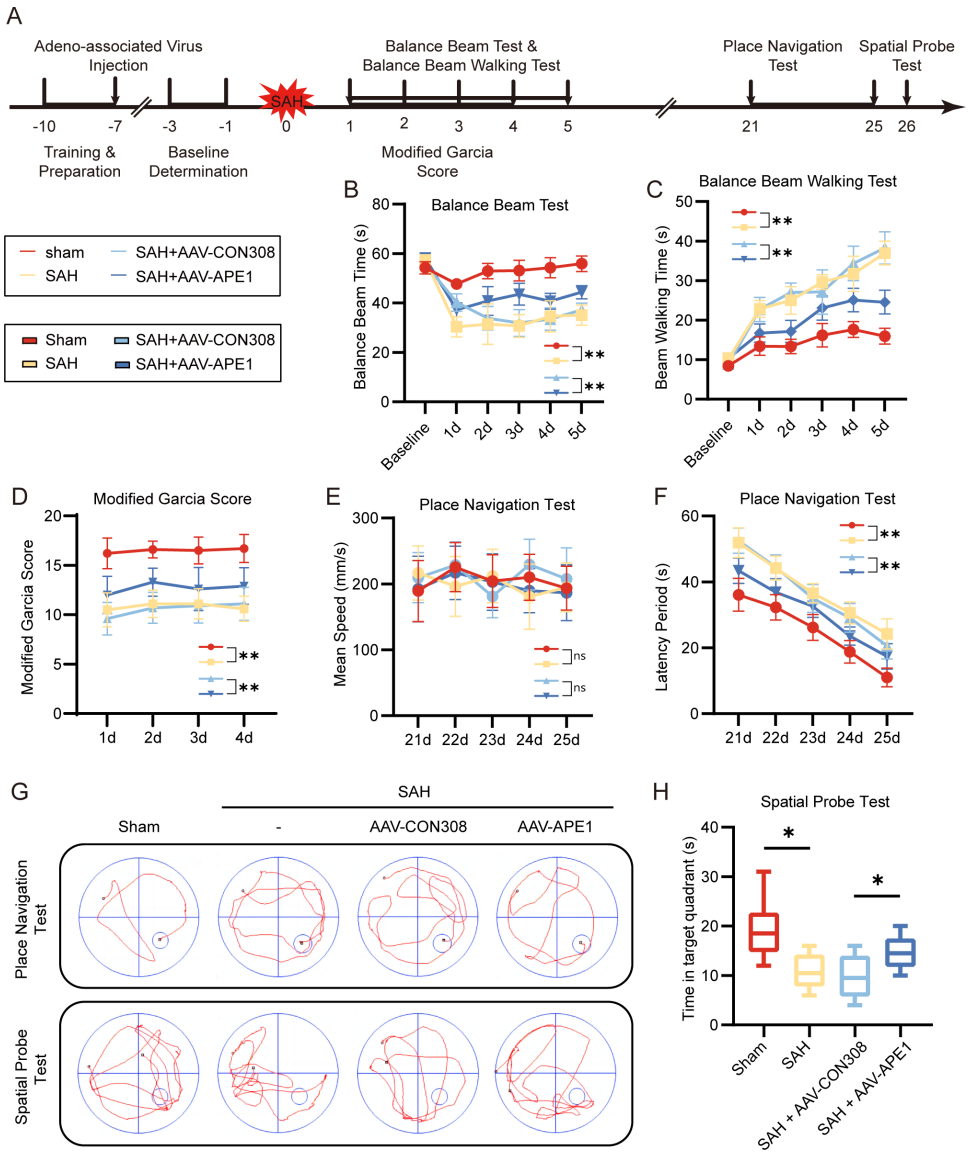

Figure 4 APE1 overexpression improved rats' neurological functions after SAH. (A) Rat neurobehavioural test flow diagram. (B) Balance beam test 1–5 days after SAH. The chart illustrates the time rats drop off the beam. (C) Balance beam walking test 1–5 days after SAH. The chart illustrates the time rats cross the beam. (D) Modified Garcia Scores evaluation after SAH. (E) Swimming speed of rats in Morris water maze test. (F) Place navigation test 21–25 days after SAH. (G) Rat swimming tracks in the place navigation test. (H) Space probe experiment 26 days after SAH. The data are expressed as mean±SD, n=10 per group. * and ** denote statistical significance at $p<0.05$ and $p<0.01$, respectively. 'ns' indicates that there was no significant difference observed. SAH, subarachnoid haemorrhage.

reflect the function of mitochondria. The result showed that neurons exposed to OxyHb decreased the ATP content, and the inhibitory effects were relieved with APE1 overexpression (figure 5C). The mitochondrial membrane potential was evaluated by using JC-1 staining. On examination, it was noted that neurons subjected to OxyHb exhibited an elevation in the proportion of JC-1 monomer (green fluorescence) to JC-1 aggregates (red fluorescence) in comparison to the control group. However, the ratio decreased on the introduction of APE1 overexpression (figure 5D). Quantitative analysis was carried out by flow cytometry. The ratios of red-to-green fluorescence emissions were quantitated to further estimate the extent of mitochondrial membrane damage. We observed a significant rise in the ratio after OxyHb intervention, whereas the ratio decreased after APE1 was overexpressed (figure 5E,F). These results suggested that APE1 overexpression can attenuate mitochondrial dysfunction and neuronal apoptosis.

APE1 overexpression improved mitochondrial OCR and altered mitochondrial permeability transition pore

We used the measurement of mitochondrial OCR (figure 6A). The results showed that neurons exposed to OxyHb induced a substantial decrease in basal respiration, ATP production, maximal respiratory, and spare respiratory capacity in comparison to the control group. Meanwhile, neurons transfected with APE1 significantly increased these tests (figure 6B–E). After OxyHb intervention, a lower

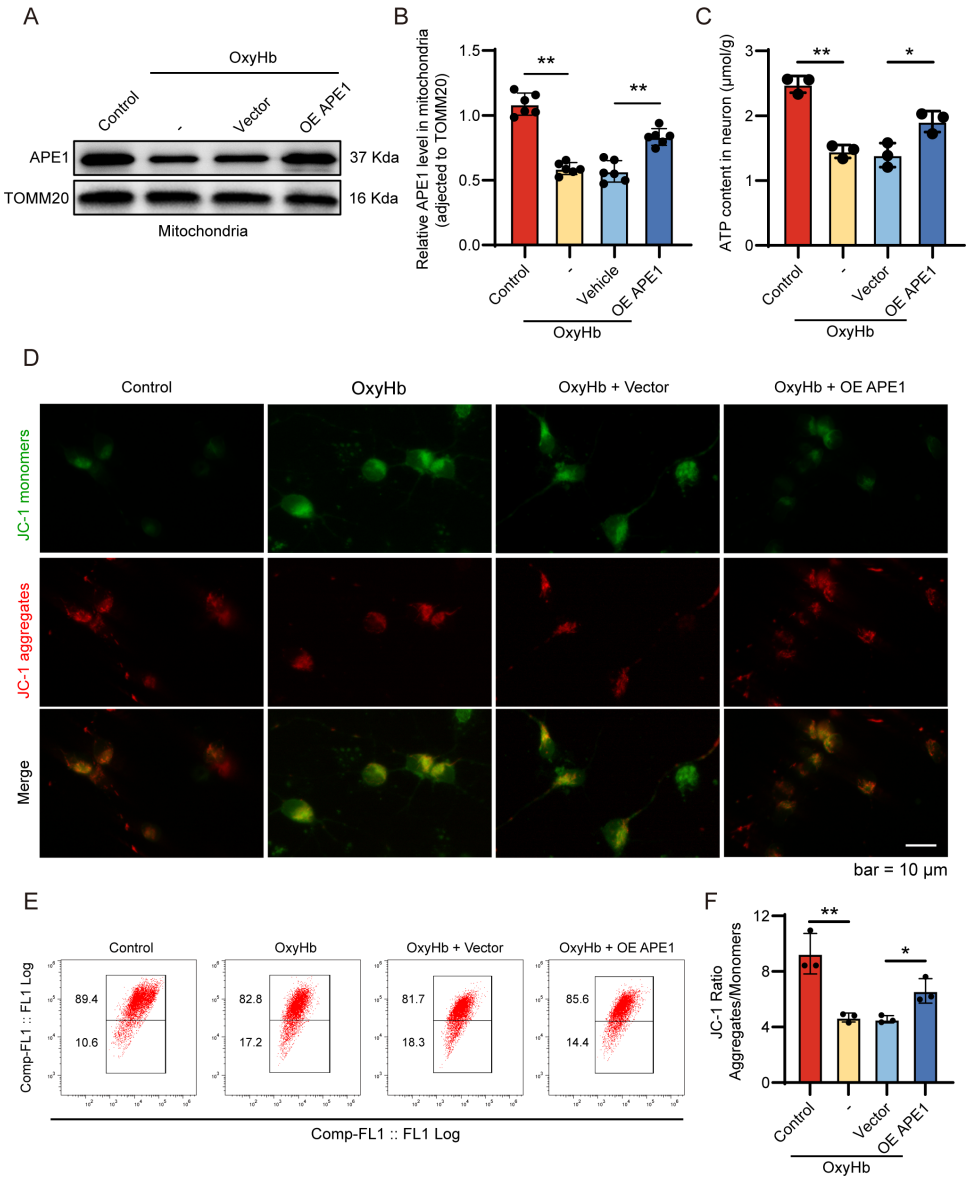

Figure 5 APE1 overexpression attenuated mitochondrial membrane potential impairment and neuronal apoptosis in vitro (A, B) APE1 protein levels in neurons transfected with overexpression plasmid by Western blot. Tomm20 as load control. (B) Presents a quantitative assessment of the APE1 level in mitochondria. Control versus OxyHb, p<0.0001. OxyHb+vector vs OxyHb+OE APE1, p<0.0001. n=6 per group. (C) ATP content of neurons. Control versus OxyHb, p<0.0001. OxyHb+vector versus OxyHb+OE APE1, p=0.0054. n=3 per group. (D) Mitochondrial membrane potential performed by JC-1 staining. Scale bar=10 μm. n=3 per group. (E) Representative images illustrate the flow cytometry detection of JC-1 in neurons at control and OxyHb groups. (F) The ratios of red-to-green fluorescence emissions were quantitated to further estimate the extent of mitochondrial membrane damage. The data are expressed in the form of mean±SD. * and ** denote statistical significance at p<0.05 and p<0.01, respectively. OxyHb, oxygenated haemoglobin.

fluorescence intensity was observed in the group, indicating a higher degree of mPTP opening. While after APE1 intervention, a higher fluorescence intensity was observed in the group, indicating a lower degree of mPTP opening (figure 6F). These results suggested that APE1 overexpression improves mitochondrial dysfunction in neurons.

APE1 participated in neuronal mitochondrial apoptosis via mitochondrial respiratory chain dysfunction

We measured the expression of γ-H2AX to investigate mtDNA damage by Western blot (figure 7A,B). The result showed that neurons exposed to OxyHb increase the expression level of γ-H2AX, and APE1 overexpression decreases the level. We conducted a Comet assay to quantify neuronal DNA damage. We observed a marked difference in the comet tail of the OxyHb intervention group compared with the control group, and the comet tail in the OE APE1 group was shorter than in the Vector group (online supplemental figure S6). In addition, to investigate mitochondrial respiratory chain function, we measured the protein expression of representative

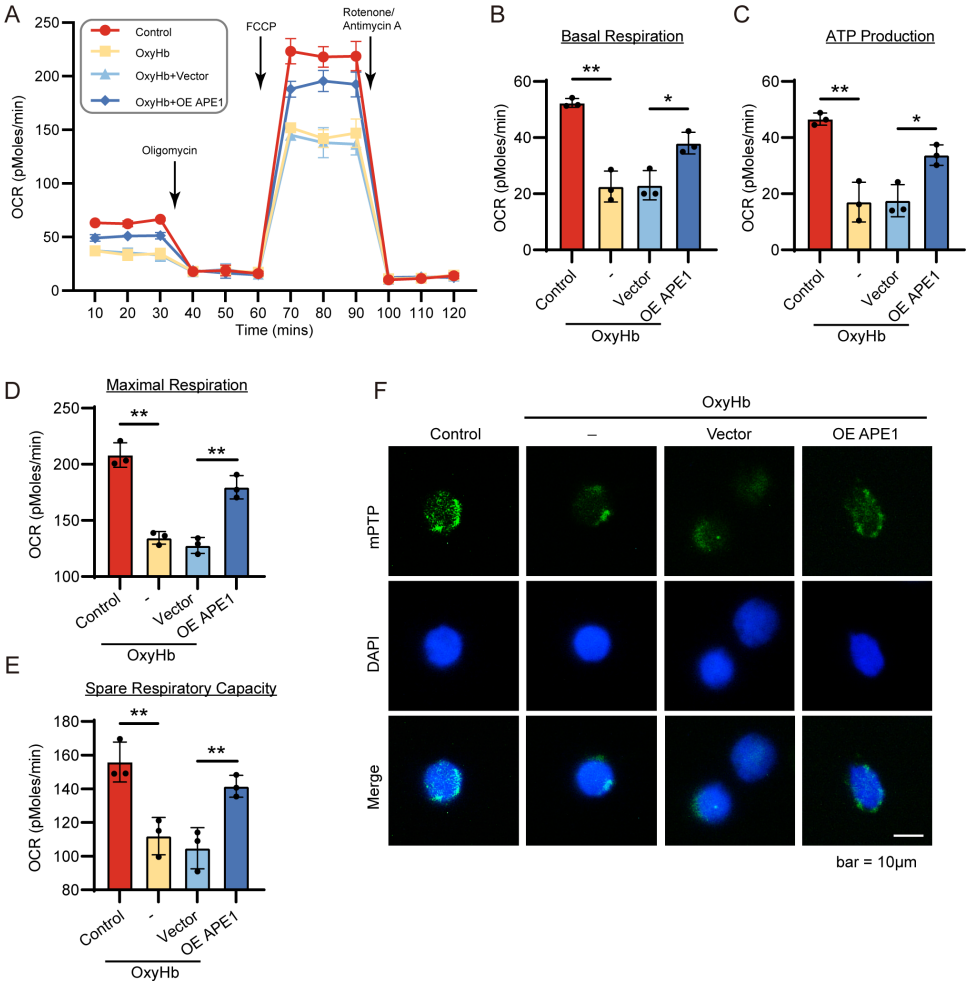

Figure 6 APE1 overexpression improved mitochondrial oxygen consumption rate and altered mitochondrial permeability transition pore (A) Effect of APE1 overexpression on mitochondrial oxygen consumption rate in neurons from the control group, OxyHb group and intervention group. OCR was measured by using the Seahorse XF-24 Extracellular Flux Analyse. (B) Effect of APE1 overexpression on Basal Respiration. Control versus OxyHb, p<0.0001. OxyHb+vector versus OxyHb+OE APE1, p=0.0056. (C) Effect of APE1 overexpression on ATP Production. Control versus OxyHb, p=0.0002. OxyHb+vector versus OxyHb+OE APE1, p=0.0084. (D) Effect of APE1 overexpression on maximal respiration. Control versus OxyHb, p<0.0001. OxyHb+vector versus OxyHb+OE APE1, p=0.0002. (E) Effect of APE1 overexpression on spare respiratory capacity. Control versus OxyHb, p=0.002. OxyHb+vector versus OxyHb+OE APE1, p=0.0058. (F) Colocalisation of mPTP (green) and DAPI (blue) within neurons of control and OxyHb groups. Scale bar=10 μm. The data are expressed as mean±SD, n=3 per group. * and ** denote statistical significance at p<0.05 and p<0.01, respectively. OCR, oxygen consumption rate; OxyHb, oxygenated haemoglobin.

subunits of mitochondrial respiratory chain complexes by Western blot. Among the 13 proteins encoded by mtDNA, we selected CYTB, MTCO2 and ATP6, which are components of the mitochondrial respiratory chain complex III, IV and V, respectively. It was observed that the neurons exposed to OxyHb displayed a decrease in the expression level of the three proteins, and the OE APE1 group manifested a significantly greater level of expression than the vector group (figure 7C–F). The expression levels of cleaved-caspase 9, a protein associated with apoptosis, were measured. The findings indicated that the OxyHb group exhibited significantly higher levels of cleaved-caspase 9 expression compared with the control group, while the OE APE1 group demonstrated downregulation of expression (figure 7G,H).

DISCUSSION

We conducted a series of experiments to explore the function of APE1 in mitochondria after experimental SAH in EBI. First, we found a marked decrease in the expression level of APE1 in the mitochondria of temporal cortex tissue following SAH. Then, we observed that mtDNA damage increased as the level of APE1 decreased. Similar results could be obtained in vitro experiments. We further found that overexpression of APE1 via AAV vector transduction increased the number of survival neurons after SAH and improved behavioural outcomes in SAH rats. In addition, overexpression of APE1 relieved energy metabolism disorders in the mitochondria of neurons and reduced neuronal apoptosis. To further explore the possible mechanism, we paid attention to the respiratory

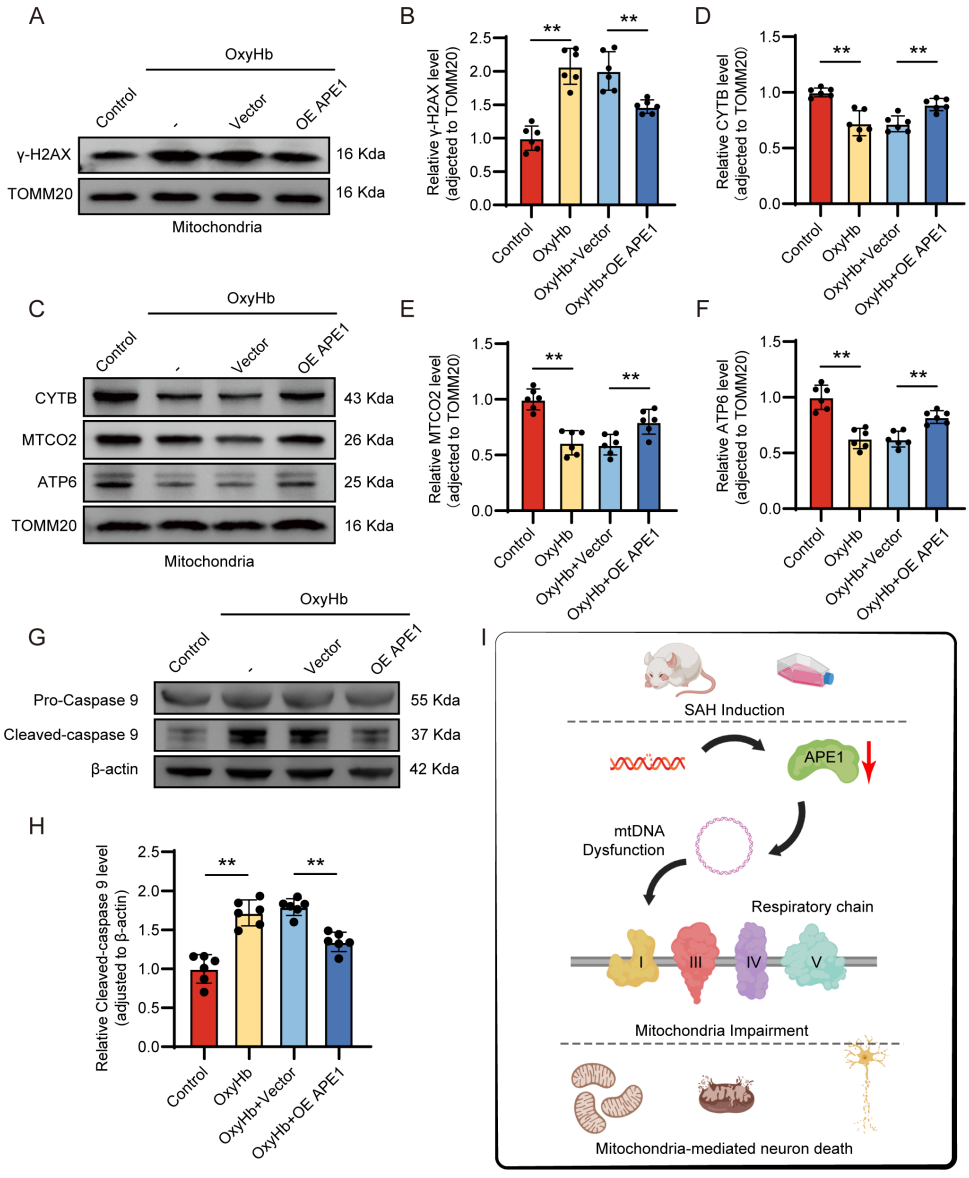

Figure 7 APE1 participated in neuronal death via mitochondrial respiratory dysfunction (A, B) γ-H2AX protein levels in neurons by Western blot. Tomm20 as load control. (B) Presents a quantitative assessment of the γ-H2AX level in mitochondria. Control versus OxyHb, p<0.0001. OxyHb+vector versus OxyHb+OE APE1, p=0.0009. (C–F) Representative subunits of mitochondrial respiratory chain complexes. Tomm20 as load control. (D) Presents a quantitative assessment of the CYTB level in mitochondria. Control versus OxyHb, p<0.0001. OxyHb+vector versus OxyHb+OE APE1, p=0.00014. (E) Presents a quantitative assessment of the MTCO2 level in mitochondria. Control versus OxyHb, p<0.0001. OxyHb+vector versus OxyHb+OE APE1, p=0.00046. (F) Presents a quantitative assessment of the ATP6 level in mitochondria. Control versus OxyHb, p<0.0001. OxyHb+vector versus OxyHb+OE APE1, p=0.0011. (G, H) Cleaved-caspase 9 protein levels in neurons by Western blot. β-actin as load control. (H) Presents a quantitative assessment of the cleaved-caspase 9 level. Control versus OxyHb, p<0.0001. OxyHb+vector versus OxyHb+OE APE1, p<0.0001. (I) The molecular mechanism of APE1 regulating neuron apoptosis. When SAH happened, the expression level of APE1 experienced a marked decrease, thereby reducing the efficiency of the BER pathway. This reduction leads to increased mitochondrial DNA damage, which affects the expression of respiratory chain subunit protein encoded by mitochondria. As a result, mitochondrial dysfunction occurs, culminating in neuronal apoptosis. The data are expressed as mean±SD, n=3 per group. * and ** denote statistical significance at p<0.05 and p<0.01, respectively. mtDNA, mitochondrial DNA; OxyHb, oxygenated haemoglobin; SAH, subarachnoid haemorrhage.

chain. We found that as the mtDNA damage increased, the protein expression of subunits of mitochondrial respiratory chain complexes decreased, and mitochondrial dysfunction occurred, culminating in neuronal apoptosis. These results indicate that APE1 plays a role in neuronal mtDNA protection and mitochondrial functional recovery after SAH via the respiratory chain (figure 7I).

SAH can lead to various complications, including mitochondrial dysfunction and DNA damage. An increase of considerable magnitude was observed in the rate of 8-OHDG positivity in immunohistochemistry experiments

conducted within the initial 24 hours following SAH in rats.[9] Mitochondria are organelles found in almost all cells that are responsible for producing energy through a process called oxidative phosphorylation. mtDNA is the genetic material that encodes the proteins necessary for this process.[11] Damage to mtDNA can impair mitochondrial function and lead to decreased energy production, increased oxidative stress, and ultimately, cell death.[11 12]

BER is a process that has been conserved throughout evolution and is able to repair endogenously and exogenously damage to the base of the DNA.[22 23] BER is a multienzyme process with two pathways, the short patch and the long patch, which is present in mitochondria as well.[22 23] The first step involves DNA glycosylase, which hydrolyzes the N-glycosidic bond between the sugar moiety and the modified base, thus creating an AP site.[24] DNA glycosylases can be either monofunctional, which only removes the modified base, or bifunctional, with an AP-lyase activity associated.[25] Bifunctional DNA glycosylase is mainly responsible for initiating the short-patch BER, while monofunctional DNA glycosylase is active in one or both of the pathways.

The upstream mechanism for the activation of BER is initiated by the recognition of the DNA lesion and subsequent recruitment of specific repair enzymes for lesion removal, incision, gap processing and gap filling.[24] DNA glycosylases are responsible for recognising specific types of damaged or incorrect bases. These glycosylases identify and remove the damaged base by cleaving the glycosidic bond between the base and the sugar in the DNA backbone.

APE1 is an essential protein with multifaceted functionality integral to DNA repair and redox signalling.[14 16] It is predominantly found in the nucleus and additionally in the mitochondria where it is an integral part of the mitochondrial BER (mtBER) pathway.[26] APE1 has a unique distribution of subcellular targeting signals, its sole mitochondrial targeting sequence is located in the C-terminal at residues 289-318, usually hidden by the intact N-terminal structure.[26] Lys299 and Arg301, identified as crucial residues, were reported to be essential for APE1's interaction with Tomm20 and its subsequent translocation to the mitochondria.[27] The study revealed that APE1 interacts with the mitochondrial import and assembly protein Mia40, implying a redox-assisted mechanism for APE1 to be transported into the mitochondria, which depends on the disulfide transfer system.[28]

ROS mainly originate from high mitochondrial respiration activity or malfunctioning organelles.[29] Researchers gain insights into the underlying mechanisms of various neurological disorders by assessing the role of APE1 in neuronal mitochondrial dysfunction.[30 31] Our research showed that APE1 is critical in protecting neurons against mtDNA damage and mitochondrial dysfunction and preventing neuronal apoptosis after SAH. Increased oxidative stress can lead to DNA damage, and APE1 plays a critical role in repairing this damage and preventing the accumulation of mutations that can lead to disease progression.[29] Previous studies revealed that the decreased expression of APE1 in mitochondria may be due to the whole protein level depletion or the protein post-translation modifications.[32 33] Our research indicated that APE1 expression decreased after SAH might be caused by depletion of total protein levels. However, the role of post-translational modification after SAH is yet to be confirmed. APE1 depletion can occur under different circumstances.[34] First, oxidative stress, which is associated with various diseases and ageing, can affect APE1 function and lead to its depletion.[32] Second, APE1 deficiency has been reported to be correlated with certain human diseases, such as amyotrophic lateral sclerosis.[35]

Besides its role in DNA repair, APE1 is also involved in several critical processes in the immune response.[36] One of the primary functions of APE1 in the immune response is the regulation of cytokine and chemokine expression through the activation of redox-sensitive transcription factors, such as NF-kB and AP-1.[37 38] Moreover, many studies have demonstrated APE1 exhibits both pro-inflammatory and anti-inflammatory effects.[39 40] The dual role of APE1 in cytokine and chemokine expression probably due to specific physiological roles reflecting different cellular context. Finally, APE1 is involved in class switch recombination, a process that is critical for the generation of antibody diversity in the immune system.[36] APE1 can interact with activation-induced cytidine deaminase (AID), which is necessary for class switch recombination to occur.[41] By regulating the activity of AID, APE1 can influence the generation of diverse antibodies and the effectiveness of the immune response.

mtDNA damage can significantly impact the function of the respiratory chain, which is the series of protein complexes responsible for generating ATP, the main energy source for cellular processes.[42 43] The respiratory chain consists of five protein complexes that are located in the inner mitochondrial membrane. Complexes I, III, IV and ATP synthase (also known as complexes V) contain multiple subunits encoded by nuclear and mtDNA, while complex II encodes solely by nDNA.[44]

Damage to mtDNA can impair the function of the respiratory chain in several ways.[45–47] First, mtDNA mutations can affect the subunits of complexes I, III, IV and V, leading to decreased activity of these complexes and reduced ATP production. A previous study has indicated that the respiratory chain impairment was associated with mitochondrial-encoded respiratory chain subunits rather than nuclear-encoded subunits.[48–50] Second, mtDNA damage can impair the production of respiratory chain subunits, leading to reduced levels of functional protein complexes. A recent study showed that in muscle biopsy specimens of dermatomyositis patients, a reduced mtDNA copy number led to lower levels of respiratory chain proteins, which were involved in the partly mtDNA encoded complexes I and IV, but not those involved in the entire nDNA encoded complex II.[51 52] In our study, we found reduced levels of APE1 after SAH resulted in increased mtDNA damage, a reduction in the subunit

of respiratory chain complex III, IV, V levels and subsequent respiratory chain dysfunction. Furthermore, mtDNA damage can also increase the production of ROS by the respiratory chain.[48 53 54] ROS are produced as a byproduct of electron transport within the respiratory chain, and excessive ROS production can cause oxidative damage to proteins, lipids and DNA, including mtDNA.[55] This creates a vicious cycle where mtDNA damage leads to increased ROS production, which in turn can cause further damage to mtDNA and the respiratory chain.[55] Overall, mtDNA damage can significantly impact the function of the respiratory chain, leading to reduced ATP production and increased ROS production. Therefore, mtDNA damage can contribute to various pathological conditions, including mitochondrial diseases, neurodegenerative diseases and ageing.

In our study, there are still some limitations. First, only male rats were used in the study. Second, further investigation is required to understand the specific way APE1 contributes to the repair of mtDNA damage. Finally, we only examined the function of APE1 in neurons after SAH in vitro experiments. However, APE1 is expressed in both neuronal and glial cells. In follow-up experiments, we intend to test these hypotheses further.

CONCLUSION

Our study suggests that APE1 is involved in SAH EBI by affecting mitochondrial apoptosis via the mitochondrial respiratory chain. Overexpression of APE1 significantly relieved energy metabolism disorders, decreased neuronal apoptosis, and attenuated neurological dysfunction after SAH. APE1 may potentially play a vital role in EBI after SAH.

Contributors All authors contributed to the study conception and design. Material preparation, data collection and analysis were performed by KD, ZoW, BG, LL, FG and XT. The first draft of the manuscript was written by KD. Writing-review and editing by ZoW and WY. Funding acquisition: ZoW. Supervision: ZoW and ZhW. All authors read and approved the final manuscript.

Funding This work was supported by the National Natural Science Foundation of China (NSFC) grant (82002643).

Competing interests None declared.

Patient consent for publication Not applicable.

Ethics approval All animal experiments were conducted with the approval (82002643) of the Animal Experiment Administration Committee of University.

Provenance and peer review Not commissioned; externally peer reviewed.

Data availability statement Data are available on reasonable request.

ORCID iD

Zhong Wang http://orcid.org/0009-0006-4215-9337

REFERENCES

1 Claassen J, Park S. Spontaneous subarachnoid haemorrhage. *Lancet* 2022;400:846–62.
2 Schneider UC, Xu R, Vajkoczy P. Inflammatory events following subarachnoid hemorrhage (SAH). *Curr Neuropharmacol* 2018;16:1385–95.
3 Chen J, Li M, Liu Z, *et al*. Molecular mechanisms of neuronal death in brain injury after subarachnoid hemorrhage. *Front Cell Neurosci* 2022;16:1025708.
4 Xu Z, Rui Y-N, Hagan JP, *et al*. Intracranial aneurysms: pathology, genetics, and molecular mechanisms. *Neuromolecular Med* 2019;21:325–43.
5 Zhang Z, Zhang A, Liu Y, *et al*. New mechanisms and targets of subarachnoid hemorrhage: a focus on mitochondria. *Curr Neuropharmacol* 2022;20:1278–96.
6 Xu P, Tao C, Zhu Y, *et al*. Tak1 mediates neuronal pyroptosis in early brain injury after subarachnoid hemorrhage. *J Neuroinflammation* 2021;18:188.
7 Fan H, Ding R, Liu W, *et al*. Heat shock protein 22 modulates NRF1/TFAM-dependent mitochondrial Biogenesis and DRP1-sparked mitochondrial apoptosis through AMPK-PGC1A signaling pathway to alleviate the early brain injury of subarachnoid hemorrhage in rats. *Redox Biol* 2021;40:101856.
8 Jorgensen A, Staalsoe JM, Simonsen AH, *et al*. Progressive DNA and RNA damage from oxidation after aneurysmal subarachnoid haemorrhage in humans. *Free Radic Res* 2018;52:51–6.
9 Lee J-Y, Keep RF, He Y, *et al*. Hemoglobin and iron handling in brain after subarachnoid hemorrhage and the effect of deferoxamine on early brain injury. *J Cereb Blood Flow Metab* 2010;30:1793–803.
10 Loftspring MC. Iron and early brain injury after subarachnoid hemorrhage. *J Cereb Blood Flow Metab* 2010;30:1791–2.
11 Stoccoro A, Coppedè F. Mitochondrial DNA methylation and human diseases. *Int J Mol Sci* 2021;22:4594.
12 Sharma P, Sampath H. Mitochondrial DNA integrity: role in health and disease. *Cells* 2019;8:100.
13 Fontana GA, Gahlon HL. Mechanisms of replication and repair in mitochondrial DNA deletion formation. *Nucleic Acids Res* 2020;48:11244–58.
14 Caston RA, Gampala S, Armstrong L, *et al*. The Multifunctional APE1 DNA repair-redox signaling protein as a drug target in human disease. *Drug Discov Today* 2021;26:218–28.
15 Xue Z, Demple B. Knockout and inhibition of APE1: roles of APE1 in base excision DNA repair and modulation of gene expression. *Antioxidants (Basel)* 2022;11:1817.
16 Whitaker AM, Freudenthal BD. APE1: a skilled nucleic acid surgeon. *DNA Repair (Amst)* 2018;71:93–100.
17 Wang X, Wang Z, Wu J, *et al*. Thioredoxin 1 regulates the pentose phosphate pathway via ATM phosphorylation after experimental subarachnoid hemorrhage in rats. *Brain Res Bull* 2022;185:162–73.
18 Ma C, Gao B, Wang Z, *et al*. GRPEL1 regulates mitochondrial unfolded protein response after experimental subarachnoid hemorrhage in vivo and in vitro. *Brain Research Bulletin* 2022;181:97–108.
19 Chimienti G, Picca A, Sirago G, *et al*. Increased TFAM binding to mtDNA damage hot spots is associated with mtDNA loss in aged rat heart. *Free Radic Biol Med* 2018;124:447–53.
20 Chimienti G, Picca A, Fracasso F, *et al*. Differences in liver TFAM binding to mtDNA and mtDNA damage between aged and extremely aged rats. *Int J Mol Sci* 2019;20:2601.
21 Pfaffl MW. A new mathematical model for relative quantification in real-time RT-PCR. *Nucleic Acids Res* 2001;29:e45.
22 Frosina G, Fortini P, Rossi O, *et al*. Two pathways for base excision repair in mammalian cells. *J Biol Chem* 1996;271:9573–8.
23 Prakash A, Doublié S. Base excision repair in the mitochondria. *J Cell Biochem* 2015;116:1490–9.
24 Banerjee A, Santos WL, Verdine GL. Structure of a DNA glycosylase searching for lesions. *Science* 2006;311:1153–7.
25 Fortini P, Parlanti E, Sidorkina OM, *et al*. The type of DNA glycosylase determines the base excision repair pathway in mammalian cells. *J Biol Chem* 1999;274:15230–6.
26 Chattopadhyay R, Wiederhold L, Szczesny B, *et al*. Identification and characterization of mitochondrial abasic (AP)-endonuclease in mammalian cells. *Nucleic Acids Res* 2006;34:2067–76.

27 Li M, Zhong Z, Zhu J, *et al*. Identification and characterization of mitochondrial targeting sequence of human apurinic/apyrimidinic endonuclease 1. *J Biol Chem* 2010;285:14871–81.
28 Barchiesi A, Wasilewski M, Chacinska A, *et al*. Mitochondrial translocation of APE1 relies on the MIA pathway. *Nucleic Acids Res* 2015;43:5451–64.
29 Zhao R-Z, Jiang S, Zhang L, *et al*. Mitochondrial electron transport chain, ROS generation and uncoupling (review). *Int J Mol Med* 2019;44:3–15.
30 Stetler RA, Gao Y, Zukin RS, *et al*. Apurinic/apyrimidinic endonuclease APE1 is required for PACAP-induced neuroprotection against global cerebral ischemia. *Proc Natl Acad Sci U S A* 2010;107:3204–9.
31 Leak RK, Li P, Zhang F, *et al*. Apurinic/apyrimidinic endonuclease 1 upregulation reduces oxidative DNA damage and protects hippocampal neurons from ischemic injury. *Antioxid Redox Signal* 2015;22:135–48.
32 Whitaker AM, Stark WJ, Freudenthal BD. Processing oxidatively damaged bases at DNA strand breaks by Ape1. *Nucleic Acids Res* 2022;50:9521–33.
33 Choi S, Joo HK, Jeon BH. Dynamic regulation of APE1/REF-1 as a therapeutic target protein. *Chonnam Med J* 2016;52:75–80.
34 Whitaker AM, Stark WJ, Flynn TS, *et al*. Molecular and structural characterization of disease-associated APE1 polymorphisms. *DNA Repair (Amst)* 2020;91–92:102867.
35 Hadi MZ, Coleman MA, Fidelis K, *et al*. Functional characterization of APE1 variants identified in the human population. *Nucleic Acids Res* 2000;28:3871–9.
36 Oliveira TT, Coutinho LG, de Oliveira LOA, *et al*. APE1/REF-1 role in inflammation and immune response. *Front Immunol* 2022;13:793096.
37 Flaherty DM, Monick MM, Carter AB, *et al*. Oxidant-mediated increases in redox factor-1 nuclear protein and activator Protein-1 DNA binding in asbestos-treated Macrophages. *J Immunol* 2002;168:5675–81.
38 Guan Z, Basi D, Li Q, *et al*. Loss of redox factor 1 decreases NF-kappaB activity and increases susceptibility of endothelial cells to apoptosis. *Arterioscler Thromb Vasc Biol* 2005;25:96–101.
39 Hu Z, Hui B, Hou X, *et al*. APE1 inhibits foam cell formation from macrophages via Lox1 suppression. *Am J Transl Res* 2020;12:6559–68.
40 Lee H-M, Yuk J-M, Shin D-M, *et al*. Apurinic/apyrimidinic endonuclease 1 is a key modulator of keratinocyte inflammatory responses. *J Immunol* 2009;183:6839–48.
41 Vuong BQ, Herrick-Reynolds K, Vaidyanathan B, *et al*. A DNA break- and phosphorylation-dependent positive feedback loop promotes immunoglobulin class-switch Recombination. *Nat Immunol* 2013;14:1183–9.
42 Gustafsson CM, Falkenberg M, Larsson NG. Maintenance and expression of mammalian mitochondrial DNA. *Annu Rev Biochem* 2016;85:133–60.
43 Lin MT, Beal MF. Mitochondrial dysfunction and oxidative stress in neurodegenerative diseases. *Nature* 2006;443:787–95.
44 Vercellino I, Sazanov LA. The assembly, regulation and function of the mitochondrial respiratory chain. *Nat Rev Mol Cell Biol* 2022;23:141–61.
45 Grünewald A, Rygiel KA, Hepplewhite PD, *et al*. Mitochondrial DNA depletion in respiratory chain-deficient Parkinson disease neurons. *Ann Neurol* 2016;79:366–78.
46 Leonard JV, Schapira AH. Mitochondrial respiratory chain disorders I: mitochondrial DNA defects. *Lancet* 2000;355:299–304.
47 Morán M, Moreno-Lastres D, Marín-Buera L, *et al*. Mitochondrial respiratory chain dysfunction: implications in neurodegeneration. *Free Radic Biol Med* 2012;53:595–609.
48 Jaeger VK, Lebrecht D, Nicholson AG, *et al*. Mitochondrial DNA mutations and respiratory chain dysfunction in idiopathic and connective tissue disease-related lung fibrosis. *Sci Rep* 2019;9:5500.
49 Frye RE, Lionnard L, Singh I, *et al*. Mitochondrial morphology is associated with respiratory chain uncoupling in autism spectrum disorder. *Transl Psychiatry* 2021;11:527.
50 Araújo GW, Beyer C, Arnold S. Oestrogen influences on mitochondrial gene expression and respiratory chain activity in cortical and mesencephalic astrocytes. *J Neuroendocrinol* 2008;20:930–41.
51 Hedberg-Oldfors C, Lindgren U, Visuttijai K, *et al*. Respiratory chain dysfunction in perifascicular muscle fibres in patients with dermatomyositis is associated with mitochondrial DNA depletion. *Neuropathol Appl Neurobiol* 2022;48:e12841.
52 DiMauro S, Schon EA. Mitochondrial respiratory-chain diseases. *N Engl J Med* 2003;348:2656–68.
53 Lebrecht D, Setzer B, Rohrbach R, *et al*. Mitochondrial DNA and its respiratory chain products are defective in doxorubicin nephrosis. *Nephrol Dial Transplant* 2004;19:329–36.
54 Cardellach F, Martí MJ, Fernández-Solá J, *et al*. Mitochondrial respiratory chain activity in skeletal muscle from patients with Parkinson's disease. *Neurology* 1993;43:2258–62.
55 Nolfi-Donegan D, Braganza A, Shiva S. Mitochondrial electron transport chain: oxidative phosphorylation, oxidant production, and methods of measurement. *Redox Biol* 2020;37:101674.